



Pacific Northwest
NATIONAL LABORATORY

Proudly Operated by Battelle Since 1965

Analysis of Technetium Ion Exchange Resin from the 200 West Pump-and-Treat Facility

September 2017

TG Levitskaia
EL Campbell
SD Chatterjee
GB Hall

DISCLAIMER

This report was prepared as an account of work sponsored by an agency of the United States Government. Neither the United States Government nor any agency thereof, nor Battelle Memorial Institute, nor any of their employees, makes **any warranty, express or implied, or assumes any legal liability or responsibility for the accuracy, completeness, or usefulness of any information, apparatus, product, or process disclosed, or represents that its use would not infringe privately owned rights.** Reference herein to any specific commercial product, process, or service by trade name, trademark, manufacturer, or otherwise does not necessarily constitute or imply its endorsement, recommendation, or favoring by the United States Government or any agency thereof, or Battelle Memorial Institute. The views and opinions of authors expressed herein do not necessarily state or reflect those of the United States Government or any agency thereof.

PACIFIC NORTHWEST NATIONAL LABORATORY
operated by
BATTELLE
for the
UNITED STATES DEPARTMENT OF ENERGY
under Contract DE-AC05-76RL01830

Printed in the United States of America

Available to DOE and DOE contractors from the
Office of Scientific and Technical Information,
P.O. Box 62, Oak Ridge, TN 37831-0062;
ph: (865) 576-8401
fax: (865) 576-5728
email: reports@adonis.osti.gov

Available to the public from the National Technical Information Service
5301 Shawnee Rd., Alexandria, VA 22312
ph: (800) 553-NTIS (6847)
email: orders@ntis.gov <<http://www.ntis.gov/about/form.aspx>>
Online ordering: <http://www.ntis.gov>



This document was printed on recycled paper.

(8/2010)

Analysis of Technetium Ion Exchange Resin from the 200 West Pump-and-Treat Facility

TG Levitskaia
EL Campbell
SD Chatterjee
GB Hall

September 2017

Prepared for
the U.S. Department of Energy
under Contract DE-AC05-76RL01830

Pacific Northwest National Laboratory
Richland, Washington 99352

Summary

The 200 West Area Pump-and-Treat (P&T) facility at the Hanford Site is a combined treatment train consisting of unit processes to remove radionuclides such as uranium (U) and technetium (Tc-99), other inorganic (nitrate and hexavalent chromium), and organic (carbon tetrachloride and trichloroethene) contaminants. The RAD building of the P&T facility removes Tc-99 and U using ion exchange chromatography, while the other inorganic and organic contaminants are removed in the facility's BioPlant portion. The original design of the ion exchange resin for Tc-99 allowed for a 3-month Tc-99 breakthrough and subsequent resin canister change out. However, no Tc-99 breakthrough was noted for 3 years. The objective of the work was to analyze spent resin to determine if there are other compounds that may interfere with Tc-99 adsorption, and to determine whether the resin was removing any I-129.

Overall, results from these analyses showed that loading of the spent P&T Purolite A530E resin with Tc-99 was small and constitutes only about 0.034% of the theoretical capacity of the resin. However, an appreciable quantity of iodine is retained on the resin. The concentrations of I-127 and I-129 on the resin were found to be about 2.5 times greater and 350 times smaller than that of Tc-99, respectively. This means that a significant amount of non-radioactive iodine is being retained on the resin, and radioactive iodine to a much lesser extent. Since the concentration ratio of I-127 to I-129 on the resin is about 1000, this may be representative of the low concentration of radioactive I-129 in the groundwater relative to the total iodine in groundwater. Further testing is warranted to investigate efficiency and selectivity of iodate retention.

Small quantities of Co-60 and U-238 were also found on the resin. Other contaminants retained on the resin in significant quantities include chromium and iron. Resin beads were found to be inhomogeneous with respect to iron when analyzed by energy-dispersive X-ray spectroscopy, with a significant concentration of iron present in the resin beads. Iron-loaded resin beads could be easily identified by their distinct orange color, which was most likely due to the Fe(III) hydroxide. Since iron was elevated in the resin, additional studies are warranted to examine whether sorbed iron interferes with TcO_4^- retention.

Acknowledgments

This document was prepared by the Deep Vadose Zone – Applied Field Research Initiative at Pacific Northwest National Laboratory. Funding for this work was provided by the U.S. Department of Energy (DOE) Richland Operations Office. The Pacific Northwest National Laboratory is operated by Battelle Memorial Institute for the DOE under Contract DE-AC05-76RL01830.

Acronyms and Abbreviations

CAWSRP	Conducting Analytical Work in Support of Regulatory Programs
DIW	deionized water
DOE	U.S. Department of Energy
DVZ-AFRI	Deep Vadose Zone – Applied Field Research Initiative
EDX	energy-dispersive X-ray spectroscopy
EPR	electron paramagnetic resonance
ESL	Environmental Sciences Laboratory
EXAFS	extended X-ray absorption fine structure
FBR	fluidized bed bioreactor
FEP	fluorinated ethylene propylene
GAC	granular activated carbon
GEA	gamma energy analysis
HASQARD	Hanford Analytical Services Quality Requirements Document
HPGe	high-purity germanium
ICP-MS	inductively coupled plasma mass spectroscopy
ICP-OES	Inductively coupled plasma optical emission spectroscopy
IX	ion exchange
LEPS	low-energy photon spectroscopy
LSC	liquid scintillation counting
NMR	nuclear magnetic resonance
P&T	pump-and-treat
PNNL	Pacific Northwest National Laboratory
PTFE	polytetrafluoroethylene
QA	quality assurance
SEM	scanning electron microscopy
XANES	X-ray absorption near edge spectroscopy
XAS	X-ray absorption spectroscopy
XFS	X-ray fluorescence spectroscopy

Contents

Summary	iii
Acknowledgments.....	iv
Acronyms and Abbreviations	v
1.0 Introduction	1
1.1 Background	1
1.2 Ion Exchange Resin.....	1
2.0 Objectives	3
3.0 Methods	4
3.1 Sample Handling	4
3.2 Resin Analysis Methods.....	4
3.2.1 Non-destructive Methods	5
3.2.2 Destructive Analysis	9
4.0 Results	12
4.1 Technetium-99 Resin Analysis	12
4.1.1 X-ray Absorption and X-ray Fluorescence Spectroscopies.....	12
4.1.2 NMR Spectroscopy	12
4.1.3 EPR Spectroscopy	15
4.1.4 Scanning Electron Microscopy	16
4.1.5 Energy-Dispersive X-ray Spectroscopy	16
4.1.6 GEA Results.....	19
4.1.7 Destructive Analysis of Resin Samples.....	20
4.1.8 IO_3^- and IO_4^- uptake by Purolite A530E.....	22
5.0 Quality Assurance.....	24
6.0 Conclusions	26
7.0 References	27

Figures

Figure 1. (A) Teflon sample holders to contain powdered or solid samples, (B) Teflon holders enclosed on either side by Kapton tape (hidden) with a second layer of Mylar tape over the Kapton, (C) samples taped to an aluminum holder using masking tape, and (D) aluminum holder heat-sealed and taped over with Kapton tape for XAFS/XANES sample collection.	5
Figure 2. Energy splitting of unpaired electrons in a magnetic field.	7
Figure 3. Wet oxidation experimental setup with off-gas collected in a DIW bubbler.	10
Figure 5. (A) Solution state Tc-99 NMR spectra per scan of the supernatants in contact with B37FT1 (blue trace) heat-treated resin and B37FR2 (black trace) untreated resin. (B) Tc-99 NMR spectra per scan of B37FR2 resin beads thoroughly rinsed with deionized water to remove any interstitial liquid compared to B37FR2 supernatant.....	14
Figure 6. EPR spectra acquired at variable temperatures for (A) B37FR2 resin; (B) B37FT1 resin; (C) Tc(VI) reference (TcO_4^{2-}); and (D) Tc(IV) reference ($\text{TcO}_2 \cdot x\text{H}_2\text{O}$) obtained by electrochemical reduction of 10 mM TcO_4^- in 5.0 M NaNO_3 , 2 M NaOH solution. Reference spectra are taken from Chatterjee et al. 2017.....	15
Figure 7. SEM images of (A) B37FR2 resin bead and (B) cross section of B37FR2 resin bead cut using a razor blade.	16
Figure 8. Straight line EDX along the cross-sectioned surface of an orange resin bead. The top left displays the frequency of select elements as the scan progresses across the bead. The top right displays the same information for all elements observed. The graph on the bottom shows the cumulative EDX spectrum across all regions of the cross-sectioned bead.	18
Figure 9. LEPS spectrum of B37FR2 untreated resin with corresponding X-ray energies from Tc-99 and I-129 present within the sample.	19
Figure 10. Raman spectroscopy of (A) 0.02 M KIO_3 and (B) 0.02 M KIO_4 in contact with 50 mg of Purolite A530E resin.	23

Tables

Table 2. Average mass percent of elements present on the surface of an orange, tan, and off-white resin bead collected from untreated B37FR2 determined by energy dispersive X-ray spectroscopy.....	16
Table 3. Average mass percent of elements observed by EDX while scanning across the surface of cross-sectioned resin beads of varying color for untreated B37FR2 resin.	18
Table 4. Activities and associated concentrations of radionuclides retained by temperature-treated and untreated Purolite A530E resin quantified by GEA. The results are expressed in Bq or μg nuclide per gram of hydrated resin.	19
Table 5. LEPS spectrum analysis for I-129 and Tc-99 for temperature-treated (B37FT1) and untreated (B37FR2) resin samples in a 10-mL count geometry. The results are expressed in Bq or μg nuclide per gram of hydrated resin.	20
Table 6. ICP-OES results for the pristine Purolite A530E in comparison to the temperature-treated B37FT1 resin and the untreated B37FR2 resin as received from the 200 West P&T facility post wet-oxidation treatment.	21
Table 7. ICP-MS results for sequential dissolution of B37FR2 and B37FT1 resin for Tc-99 and I-129.	22

1.0 Introduction

1.1 Background

Production of plutonium for nuclear weapons has led to an estimated release of 450 billion gallons of radioactive and hazardous waste to the subsurface at the Hanford Site in Southeastern Washington State. Release of this waste has caused extensive vadose zone contamination as well as multiple groundwater plumes that cover 150 square miles beneath the site. The 200 Area at the Hanford Site, known as the Central Plateau, is divided into east, west, and north areas. The 200 Area makes up about 75 square miles and historically had the function to recover plutonium and uranium from nuclear fuel rods. As such, this portion of the site, which consists of the 200 East and 200 West Areas, contain most of the legacy solid and liquid waste contaminants of concern. Groundwater contamination beneath the 200 West Area represents a complex mixture of inorganic, radionuclide, and organic contaminants.

In June of 2012, CH2M Hill Plateau Remediation Company completed construction of a 2500-gpm pump-and-treat (P&T) system designed to remove technetium-99 (Tc-99), carbon tetrachloride, trichloroethene, nitrate, and total and hexavalent chromium from incoming groundwater. Operation of the 200 West Area P&T facility was initiated in August of 2012. The facility consists of two buildings: a RAD building and a biological treatment building. Radionuclide-containing groundwater is pumped across the Central Plateau into the RAD building at a maximum flow rate of 600 gpm, where an ion exchange (IX) system removes Tc-99. Treated groundwater from this facility is then mixed with groundwater pumped from wells with no radioactive constituents in an equalization tank. Mixed groundwater is then pumped into two parallel, fluidized bed bioreactors (FBRs) seeded with granular activated carbon (GAC), a carrier material that supports the growth of microbes.

1.2 Ion Exchange Resin

Technetium-99, one of the contaminants of concern, is produced from the fission of uranium-235 during operation of a nuclear reactor. As such, a significant amount of Tc-99 was disposed of together with nuclear waste on the Hanford Site. In oxidizing conditions, Tc-99 is predominantly present as the soluble pertechnetate anion (TcO_4^-). With a half-life of 210,000 years, coupled with the high mobility of pertechnetate in subsurface systems, the potential for bioaccumulation and toxicological effects in both plants and animals necessitates the removal of Tc-99 from the contaminated subsurface (Bonnesen et al. 2000).

The use of IX resins for water treatment is a well-developed methodology, capable of operating at relatively high flow rates, with high capacity and selectivity (Gu et al. 2007). The 200 West P&T facility uses IX technology for the removal of radionuclides, specifically, technetium and uranium, prior to biological treatment to remove remaining contaminants of concern before injection back into the aquifer (Breedlove et al. 2011).

Commercial Purolite A530E IX resin, which is highly selective for TcO_4^- and robust in large-scale separation processes, was implemented in the 200 West P&T facility to capture and remove Tc-99 from contaminated groundwater plumes. Purolite A530E is a bifunctional anion-exchange with triethylammonium and trihexylammonium exchange sites on polystyrene backbone cross-linked with

divinyl-benzene, designed for the removal of hydrophobic anions such as perchlorate and pertechnetate (Gu et al. 2005).

Combination of the two differently sized trialkylammonium groups allows higher sorptive capacities and improved kinetics. The hydrophilic trihexylammonium sites have a bias for sorption of large, poorly hydrated anions, such as pertechnetate, whereas the more hydrophilic triethylammonium group facilitates faster kinetics (Bonnesen et al. 2000). This balance between selectivity and uptake kinetics with Purolite A530E anion-exchange resin allows the selective removal of ClO_4^- and TcO_4^- in the presence of other anions encountered in groundwater at significantly higher concentrations (Bonnesen et al. 2000; Valenta et al. 2010).

The 200 West P&T facility uses Purolite A530E IX resin to capture Tc-99 from seven wells, which contain concentrations of Tc-99 greater than the federal drinking water limit of 900 pCi/L, prior to the centralized treatment system for processing of carbon tetrachloride and other contaminants of concern (Breedlove et al. 2011). The high selectivity and theoretical loading capacity of Purolite A530E of 0.6 equivalents/L allows processing of very large volumes of groundwater without replacement. Prior to disposition, the spent resin will be subjected to heating to strip off weakly adsorbed halogenated organics. Purolite A530E resin is reported to be able to withstand temperatures up to 100 °C, making this resin advantageous due to thermal stability, operability, and commercial availability. Previous studies on the stability of loaded Purolite A530E resin indicate that release of Tc-99 from the resin (at temperatures below 80 °C) is less than 0.02% of total Tc-99 loaded, suggesting the heat treatment of the resin will have negligible impact on Tc-99 retention (Valenta et al. 2010).

2.0 Objectives

Two representative samples of the homogenized loaded Tc-99 IX Purolite A530E resin were obtained from the 200 Area P&T facility. One sample was subjected to thermal treatment for removal of chlorinated organics, while the other sample remained untreated.

The objectives of this work were to

1. evaluate effective Tc-99 loading on the Purolite A530E resin and determine if low-valent Tc-99 species in addition to pertechnetate are retained by the resin; and
2. determine what other radioactive (e.g., I-129, Co-60) or hazardous (e.g., heavy metals) contaminants are retained on the resin.

To meet these objectives, experiments were carried out using a combination of (1) a wide range of non-destructive analytical techniques for direct evaluation of the oxidation state and coordination environment of Tc-99 retained on the IX resin and (2) destructive analysis of the IX resin using wet oxidation to identify contaminants retained by the resin. This report characterizes the chemical composition of technetium removed by Purolite A530E and the effect of temperature treatment on retaining Tc-99 among co-contaminants on the resin used at the 200 West P&T facility.

3.0 Methods

Resin samples for the laboratory analyses were collected by CH2M Hill Plateau Remediation Company during a variety of operations at the 200 West P&T facility. Sample handling upon arrival at Pacific Northwest National Laboratory (PNNL) facilities is described in Section 3.1. The laboratory analysis methods used for the resin are presented in Section 3.2.

3.1 Sample Handling

After 3 years of receiving Tc-99 laden groundwater, lead IX resin canisters at the 200 West P&T facility were taken out of service and replaced. One untreated sample was taken from the resin canister and sent to PNNL for analysis. A second sample that had been heat-treated to remove any chlorinated volatile organic carbon was also taken and sent to PNNL for analysis. These two samples of Purolite A530E resin (B37FR2 and B37FT1), designating untreated and temperature-treated resin, respectively, were received from the 200 West P&T facility. Both samples varied in color and resin bead size. According to the vendor, particle sizes range from 300 to 1200 μm . The color of the resin beads varied from off-white to tan, grey, and even orange, with no visible difference between the temperature-treated resin and the untreated resin upon receipt of the samples. After an extended period, the mother liquor of the untreated B37FR2 resin sample formed green mold against the sides of the plastic storage bottle, but the resin beads themselves appeared visibly unaltered.

Pristine Purolite A530E resin procured from the manufacturer (Purolite) was used as a control for destructive analyses to understand chemical constituents present from resin manufacturing steps or inherent to the polystyrene/divinyl-benzene resin framework. This non-radioactive resin was also used in the development of the wet oxidation method used for dissolution of the temperature-treated and untreated resin samples.

3.2 Resin Analysis Methods

Direct evaluation of the technetium environment on the Purolite A530E resin was examined using X-ray absorption near edge spectroscopy (XANES) and nuclear magnetic resonance (NMR) spectroscopy. Non-destructive analytical techniques including gamma energy analysis (GEA) and low-energy photon spectroscopy (LEPS) were incorporated to quantify radionuclides retained on the resin. Scanning electron microscopy (SEM) and energy-dispersive X-ray spectroscopy (EDX) were used to visually inspect the IX beads and quantify chemical constituents on the surface and penetration through the bead.

Destructive analysis of the resin was explored through wet oxidation to identify and quantify co-contaminants sorbed to the IX resin. Inductively coupled plasma optical emission spectroscopy (ICP-OES) and ICP-mass spectrometry (ICP-MS) were used to analyze for metals and specific isotopes retained on the resin, including Tc-99 and U-238.

3.2.1 Non-destructive Methods

3.2.1.1 X-ray Absorption Near Edge Structure Spectroscopy

XANES data were obtained at the Advanced Photon Source (APS) BL-12 BM in fluorescence mode at Argonne National Laboratory. For the collection of X-ray absorption (XAS) and X-ray fluorescence (XFS) spectroscopies, sub-samples of the B37FR2 and B37FT1 resin beads were removed from the mother liquor, washed three times with 18 M Ω deionized water (DIW), and allowed to dry. The dried resin beads were ground into fine powder using a mortar and pestle, and each of the resins was separately loaded into Teflon holders enclosed on either side by Kapton tape as shown in Figure 1. An additional layer of Mylar taper was placed over the Kapton tape and the samples were secured to an aluminum holder. The aluminum holder was placed into a transparent Mylar hot seal bag and the seal was taped over with Kapton tape to ensure full containment of radioactive material.

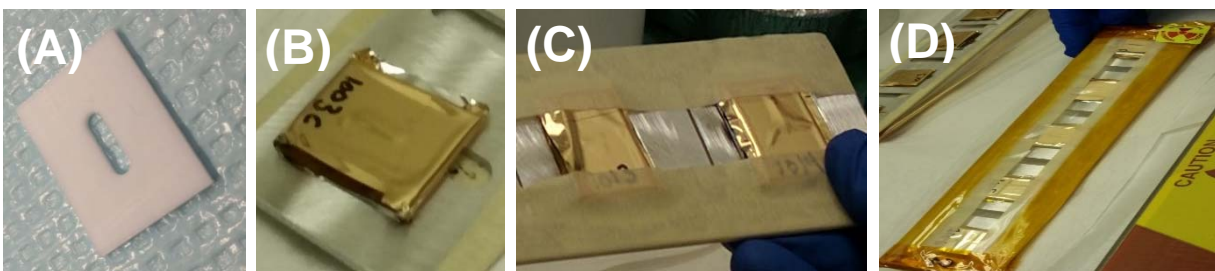


Figure 1. (A) Teflon sample holders to contain powdered or solid samples, (B) Teflon holders enclosed on either side by Kapton tape (hidden) with a second layer of Mylar tape over the Kapton, (C) samples taped to an aluminum holder using masking tape, and (D) aluminum holder heat-sealed and taped over with Kapton tape for XAFS/XANES sample collection.

XANES data were obtained from 200 eV below the Tc K-edge to 1000 eV above the edge; the data from 75 eV below the edge to 200 eV above the edge were obtained with 0.5 eV spacing. The rest of the data points are widely spaced (50 eV) and were used for the pre- and post-edge correction. The monochromator was detuned 50% to reduce the harmonic content of the beam. Fluorescence data were obtained using a 100 element Ge detector and were corrected for detector dead time. Data were converted from raw data to spectra using SixPack (Rehr et al. 1992). Spectra were normalized using Artemis, to process raw data (Lukens et al. 2002). XANES standard spectra were carefully energy calibrated using TcO₄⁻ adsorbed on Reillex-HPQ as the energy reference.

3.2.1.2 Technetium-99 Nuclear Magnetic Resonance Spectroscopy

NMR analysis for Tc-99 in the samples was performed in the Radiochemical Processing Laboratory (RPL) at PNNL. The resin sub-samples or mother liquor solution aliquots used for Tc-99 NMR analyses were placed in capped polytetrafluoroethylene (PTFE)/fluorinated ethylene propylene (FEP) copolymer sleeves (Wilma Lab Glass, Vineland, NJ), which were then inserted into 5- or 10-mm glass NMR tubes to provide secondary containment for the radioactive liquid. Tc-99 NMR data were routinely collected at 67.565 MHz on a Tecmag Discovery spectrometer equipped with a 10-mm broadband Nalorac probe as described previously (Cho et al. 2004). A solution containing 10 mM TcO₄⁻ was used as a Tc-99 chemical shift reference, and all chemical shift data are quoted relative to TcO₄⁻ (Franklin et al. 1982).

The B37FR2 resin sample was analyzed by Tc-99 NMR. A 3-mL aliquot of the resin was removed from the mother liquor and thoroughly rinsed with DIW. Pristine A530E resin was loaded with TcO_4^- to use as a reference for Tc-99 NMR. Nominally 3 mL of dry, pristine resin was contacted with 5 mL of 0.02 M TcO_4^- solution in DIW on a shaker table for 24 hours. Aliquots of the initial (0.02 M) TcO_4^- solution and the supernatant after 24 hours of contact with Purolite A530E were counted by liquid scintillation counting (LSC) to quantify uptake of TcO_4^- on Purolite A530E from DIW. LSC results indicate quantitative uptake (>99.9%) of TcO_4^- by Purolite A530E with 0.02 M TcO_4^- loaded onto the pristine resin from DIW as a reference for Tc-99 NMR. The B37FR2 and TcO_4^- -loaded control resin samples suspended in the DIW were loaded in the NMR tube for analysis as described above.

3.2.1.3 Electron Paramagnetic Resonance Spectroscopy

Electron paramagnetic resonance (EPR) analysis was performed in the Environmental Molecular Sciences Laboratory (EMSL) at PNNL. The B37FR2 and B37FT2 resin samples were aliquoted (about 10 mg), thoroughly rinsed with DIW, and placed in the 3.15-mm inside diameter liners and 5-mm outside diameter tubes for EPR measurements. EPR spectra were acquired on a Bruker EMX spectrometer equipped with an ER4102ST resonator (spectra at room temperature and 120 K) or on an ER4116DM Dual Mode resonator (spectra at 5 K) and an Oxford ESR910 cryostat. Samples were doubly contained by employing unbreakable FEP tube liners (Wilmad) inside traditional quartz EPR tubes. The spectra were collected at in the temperature range of 125 to 2 K. Hyperfine constants and g-values were extracted from the spectra via least squares fitting of the spectra with the EasySpin software package (Stoll and Schweiger 2006).

3.2.1.4 Scanning Electron Microscopy and Energy-Dispersive X-ray Spectroscopy

SEM and EDX were performed on resin beads representative of the bulk sample of B37FR2 to examine chemical constituents sorbed to the surface and throughout the cross-section of the resin. Resin beads were selected based on color with inclusion of an off-white bead, a tan bead, and an orange bead subjected to analysis on the surface of the bead.

The resin beads were mounted on a carbon-tape-coated SEM stub. The samples were then carbon coated and placed in the instrument chamber. Resin beads were imaged on a FEI Helios NanoLab 660 FIB/SEM at different voltages. SEM/EDX analyses were performed in RPL.

EDX is an analytical technique used for elemental analysis or chemical characterization of a sample. An X-ray beam is used to excite electrons within the inner shell of atoms within the sample, ejecting the electron from the shell and creating an electron hole. An electron from an outer, higher-energy shell then fills the hole and the difference in energy from the higher energy shell and the lower energy shell is emitted as an X-ray. The energies of these X-rays are characteristic of the atomic structure of the emitting element, which allows for elemental composition of the sample to be determined. The EDX line scans for B37FR2 resin beads were performed with an EDAX Octane Silicon Drift Detector and the percent mass for each element was calculated against total elemental composition.

EPR spectroscopy is a method for studying materials with unpaired electrons (Odom et al. 2006). The basic concepts of EPR are analogous to those of NMR, but here electron spins that are excited instead of

the spins of atomic nuclei in the NMR technique. The energy of an unpaired electron is given by the relation:

$$E = m g_e \mu_B B_0$$

where g_e is the Landé g factor, μ_B is Bohr magneton, m_s is the magnetic moment and is equal to $+1/2$ or $-1/2$ depending on whether the electron is oriented antiparallel or parallel to the external magnetic field, and B_0 is the field strength of an external magnetic field. Therefore, the separation between the lower and the upper states for unpaired free electrons is given by the relation:

$$\Delta E = g_e \mu_B B_0$$

The unpaired electron can move between the two energy levels by either absorbing or emitting a photon of energy $h\nu$ such that the resonance condition $h\nu = g_e \mu_B B_0$ is obeyed Figure 2.

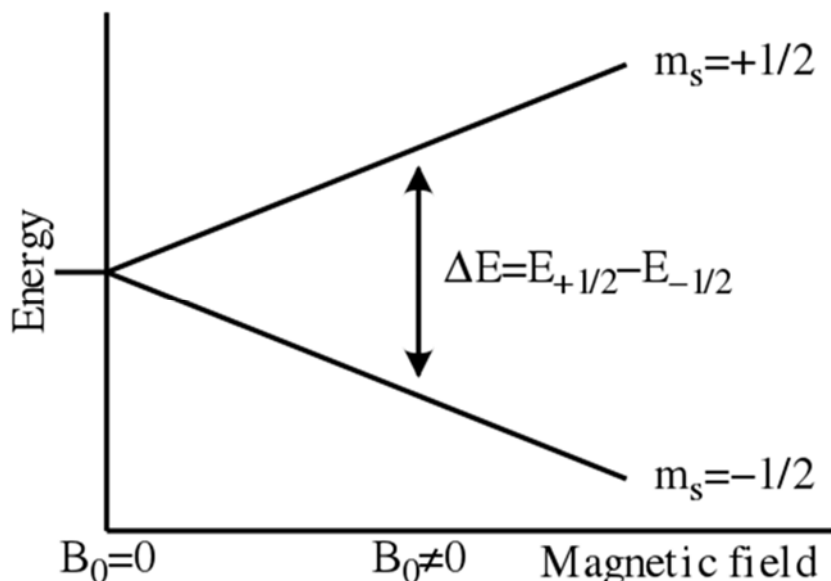


Figure 2. Energy splitting of unpaired electrons in a magnetic field.

Tc species in the even oxidation states II, IV, and VI are paramagnetic and have an outer electron configuration of $4d^5$, $4d^3$, and $4d^1$, respectively, and therefore the EPR method can be used for their determination. The EPR spectrum arising from a Tc-99-containing species exhibits characteristic fine splitting into 10 lines due to a nuclear spin of $9/2$ attributed to the Tc-99 nucleus. The resulting Tc EPR spectrum is easily distinguishable from the spectral profiles due to the paramagnetic transition metals. Tc(II) and Tc(VI) species demonstrate slow relaxation from the excited to ground state and generate EPR spectra at temperature of around 125 K. This provides means for their differentiation from Tc(IV) species that exhibit EPR signal at liquid He temperatures of less than 4 K due to very fast relaxation, requiring extremely lower temperatures for their detection (Lukens et al. 2002).

To investigate whether sorption of elements by the resin beads was a surface phenomenon or if elements were penetrating to the core of the resin bead, the resin beads were cross-sectioned using a razor, and then EDX analysis was performed in a straight line across the cross-sectioned face of the resin

beads. In total, three beads were examined in this manner. The three cross-sectioned beads had colors of off-white, orange, and gray.

3.2.1.5 Gamma Energy Analysis and Low-Energy Photon Spectroscopy

Subsamples of the B37FR2 and B37FT1 resin beads were rinsed three times with Tc-99 to remove any interstitial contaminants and remaining supernatant. After rinsing, all water was decanted from the resin beads, but the beads remained hydrated. Resin samples were aliquoted into 20-mL plastic scintillation vials to achieve a 10-mL calibrated geometry for γ counting. The corresponding masses of the B37FR2 and B37FT1 wet resin beads were 10.522 and 10.241 g, respectively.

The samples were counted on two high-purity germanium (HPGe) detectors: “Y” and “Z”. The detectors are Canberra p-type coaxial model GC10021 detectors of nominal 100% relative efficiency in a vertical cryostat configuration with a 30-L liquid nitrogen dewar. Each detector is located in a Gamma Products low background lead cave (4 inches thick) with a graded copper and tin liner. The detectors are connected to Canberra Lynx digital signal processors, which provide bias voltage, pulse processing, and an multichannel analyzer functions. The Lynx are controlled and the spectra analyzed with the Canberra Genie 2000 Gamma Spectroscopy software suite (G2K v1.3.2) running in the Apex 1.3 control environment. The gamma detectors are calibrated from 46 to 1836 keV energy range using multi-isotope standards that are NIST traceable. Control sources containing Am-241, Cs-137, and Co-60 are analyzed before the use of the detectors to confirm proper detector and pulse analysis operation.

The samples were counted on the detector face or “P0” position and also at the “P3” position, 7 cm from the detector face. The remote geometry count was performed as a check on the “P0” results due to the relatively high Tc-99 content and the resulting large beta continuum in the lower energy region of the gamma spectrum (i.e., the 89.5 keV).

For gamma counting, the uncertainty in the counting data, photon abundance and the nuclear half-life, and efficiency are included in the calculation of the total uncertainty along with a systematic uncertainty for sample preparation. It is conservatively assumed that 2% is the lowest uncertainty possible for GEA measurements while accounting for systematic uncertainties in gamma calibration standards. While the sample geometry – 10 g of resin in a 20-mL plastic scintillation vial – is not identical to the detector calibration geometry of 10 mL of aqueous standard in a standard 20-mL plastic scintillation vial, the difference is not thought to introduce a large uncertainty into the results. Overall GEA results can be assumed to have a 5% relative uncertainty at 1 sigma.

The lowest calibration point for the GEA detectors is 46 keV from Pb-210. Because of that and the thickness of the germanium dead layer on the GEA detectors, quantification of gamma and X-rays below 40 keV is difficult and is not routinely performed with p-type coaxial HPGe detectors.

To quantify lower-energy gamma and X-rays, the samples were counted on a Canberra GL2015R low energy detector (LEPS-2). The detector consists of 15-mm-thick HPGe crystal with a thin (0.3-mm) dead layer and 0.6 mm carbon fiber window allowing propagation/transmission of the low-energy photons with minimal interaction of higher energy gamma and X-rays. A calibration was performed with multi-isotope standard prepared with 10 mL of aqueous standard added to a 20-mL standard plastic scintillation vial. The vials were individually bagged, similar to the resin samples, and were counted on LEPS-2 at the “P4”

position, approximately 1 inch from the detector face. The resin samples were counted at the same position as the individual calibration vials.

3.2.1.6 Raman Spectroscopy for IO_3^- and IO_4^- Uptake

Raman spectroscopy was used to monitor selectivity and uptake of IO_3^- and IO_4^- with pristine Purolite A530E resin. One milliliter of 0.02 M KIO_4 or 0.02 M KIO_3 was added to approximately 50 mg of dry Purolite A530E resin in a half dram vial. The solution was stirred for approximately 5 minutes, centrifuged, and then analyzed using Raman spectroscopy. This was performed using a 670-nm laser and InPhotonics RS2000 high-resolution spectrometer equipped with a thermoelectrically cooled charged coupled device; detector operating at -55°C ; a 670-nm, 150-mW diode laser as the excitation source; and focused fiber optic probe RamanProbe operated in a 180° back reflection mode. Spectra were processed with Molecue software. An average of 10 scans were selected with 10-second integration time, and spectral window from 400 to 4000 cm^{-1} . Raman spectra of 0.02 M KIO_3 and KIO_4 prior to contact with the resin and DIW were taken for reference and baseline corrected using OMNIC software. The DIW spectrum was subtracted from the reported spectrum for calculation of IO_3^- and IO_4^- uptake.

3.2.2 Destructive Analysis

3.2.2.1 Ion Exchange Resin Wet Oxidation

To determine what other contaminants in addition to Tc-99 are retained by the P&T Purolite A530E resin, a series of resin digestion experiments were conducted to destroy the resin by wet oxidation and analyze the digestion solution by ICP. This technique also allows quantification of the total amount of Tc-99 retained on the Purolite A530E resin to verify radiochemical analysis results.

Combinations of oxidizers, such as $\text{HNO}_3 + \text{H}_2\text{O}_2$, $\text{HNO}_3 + \text{HCl}$, and $\text{H}_2\text{SO}_4 + \text{H}_2\text{O}_2$, were investigated using hydrated, pristine Purolite A530E resin beads as a control. Upon gentle heating and stirring, 4 mL of a 3:1 mixture of concentrated H_2SO_4 and H_2O_2 (commonly known as Piranha solution) successfully dissolved nominally 250 mg of the hydrated pristine resin. However, during attempts to dissolve the received P&T resin samples, the resin beads and solution turned dark brown, but did not dissolve. The liquid was analyzed for β -emitting radionuclides using LSC on a PerkinElmer Tri-Carb 3100 instrument and sufficient activity was detected in the solution, indicating removal of the radioactive contaminants from the loaded resin. Dilution factors necessary to analyze Piranha solution by ICP-OES and/or ICP-MS resulted in concentrations of analytes of interest under detection limit. Thus, a new avenue for wet oxidation using $\text{HNO}_3 + \text{H}_2\text{O}_2$ was explored.

Dry, pristine Purolite A530E resin used as a control sample was hydrated with 18 M Ω of Tc-99. Approximately 250 mg of the rinsed B37FR2 and B37FT1 resin samples were massed into 40-mL glass scintillation vials for analysis.

A rubber stock cock was placed atop the 40-mL scintillation vial with tubing connecting to a bubbler containing a known volume of 18 M Ω DIW. A needle was used for pressure relief in the bubbler system as shown in Figure 3. The water bath was maintained at approximately 100°C throughout the wet oxidation.

One milliliter of concentrated HNO_3 was added to the ~250-mg sample of resin. The reaction system was heated with vigorous stirring for 30 minutes, removed from the water bath, and cooled to room temperature. The reaction vial filled with NO_x gas upon heating. Once the reaction vial cooled to room temperature, 1 mL of 30% H_2O_2 was added to the vial and it was heated in the water bath for an additional 30 minutes. The solution was cooled to room temperature and transferred to a 5-mL volumetric flask. The resin beads were rinsed with DIW and the rinses were combined in the 5-mL volumetric flask and taken up to volume with DIW. The water from the bubbler was collected and diluted to volume in a 10-mL volumetric flask with DIW.

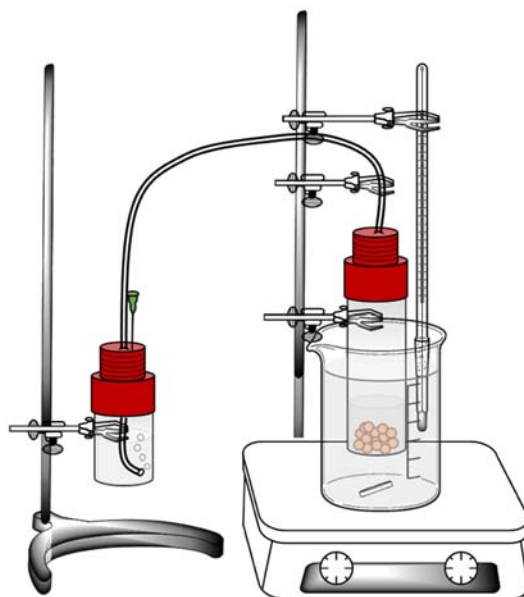


Figure 3. Wet oxidation experimental setup with off-gas collected in a DIW bubbler.

The digested resin samples were subjected to the second digestion procedure to remove additional constituents remaining on the resin. LSC counts of the second dissolution step had detectable activity, validating the need for the second digestion step. Based on LSC counts after one dissolution step, only ~65% of the total activity was removed, with an additional ~35% removed during the second dissolution step. After the final digestion, the resin beads changed from tan and brown to a uniform orange color and the $\text{HNO}_3 + \text{H}_2\text{O}_2$ reaction solution was opaque yellow. Duplicate samples were taken for the control Purolite A530E, B37FR1, and B37FT2.

3.2.2.2 Inductively Coupled Plasma Analysis

The bubbler and the leaching solution were analyzed for the metal panel using a PerkinElmer 8300DV inductively coupled plasma-optical emission spectrometer using procedure PNNL-ESL-ICP-OES, *Inductively Coupled Plasma-Optical Emission Spectrometry (ICP-OES) Analysis* (PNNL 2016a). High-purity calibration standards were used to generate calibration curves and a separate standard source to verify continuing calibration during the analytical run. Serial dilutions were made to investigate and correct for matrix interferences. This method is similar to EPA SW-846 Method 6010C, *Inductively Coupled Plasma-Atomic Emission Spectrometry* (EPA 2007a).

Analysis of trace elements, including I-127, Tc-99, and U-238, was performed using a PerkinElmer ELAN DRC-II inductively coupled plasma-mass spectrometer using procedure PNNL-ESL-ICPMS, *Inductively Coupled Plasma Mass Spectrophotometry (ICP-MS) Analysis* (PNNL 2016b). High-purity calibration standards were used to generate calibration curves and a separate standard source to verify continuing calibration during the analytical run. Serial dilutions were made to investigate and correct for matrix interferences. This method is similar to EPA SW-846 6020A, *Inductively Coupled Plasma-Mass Spectrometry* (EPA 2007b).

4.0 Results

4.1 Technetium-99 Resin Analysis

4.1.1 X-ray Absorption and X-ray Fluorescence Spectroscopies

A combination of XAS and XFS can unequivocally determine the oxidation state of a metal center, and possibly can be useful in the identification of the coordination and binding environment around the metal center through a non-destructive analysis.

The non-treated B37FR2 resin generated Tc K-edge XAS spectrum with a distinct profile at 21044 eV as shown in Figure 4. Comparison with the reference spectrum corresponding to TcO_4^- indicates the Tc K-edge characteristic of the +7 oxidation state so that TcO_4^- is the dominant Tc-99 species loaded on the P&T Purolite resin. There was no Tc-99 signal observed by XAS for the heat-treated sample, which was attributed to the attenuation of the photon beam by this particular sample configuration.

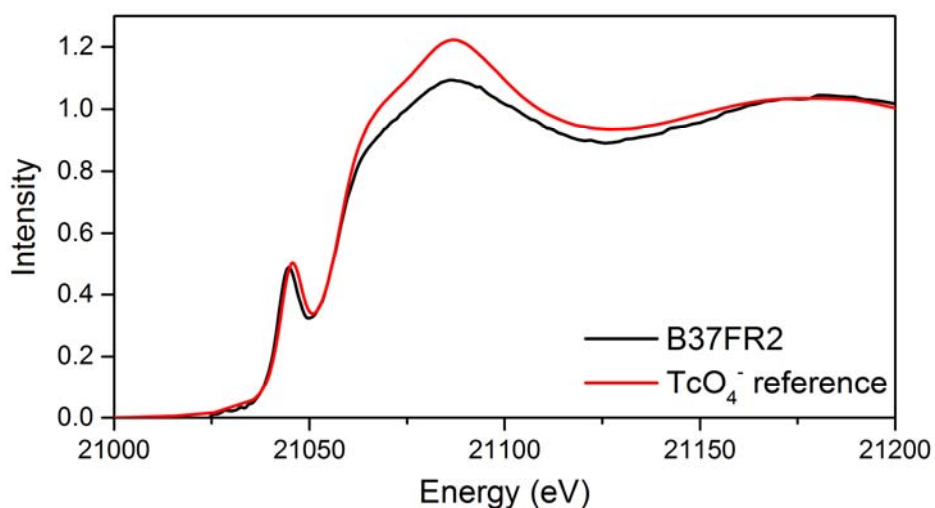


Figure 4. Tc K-edge XANES spectrum from the powdered B37FR2 untreated resin overlaid with Purolite A530E loaded with TcO_4^- from a groundwater matrix as a reference.

4.1.2 NMR Spectroscopy

NMR spectroscopy looks at the transition of a nuclear spin in a magnetic field from a low energy state in line with the magnetic field to a high energy state opposing the magnetic field. When placed in a magnetic field, NMR active nuclei (such as H-1, C-13, or Tc-99) absorb electromagnetic radiation at a frequency characteristic of the isotope. The excited nuclei subsequently emit this radiation in the form of a nuclear free induction decay, which is characteristic not only of the nuclei but is influenced by the electronic environment around them as well. This influence arises from the fact that upon application of an external magnetic field, the electrons in the vicinity of a nucleus move in response to the magnetic field and create a local magnetic field that oppose the stronger external magnetic field. This local field, therefore, “shields” the nuclei from the external magnetic field, which therefore needs to be raised to

obtain the required excitation radiofrequency. Different electronic environments can result in different amount of shielding, which is reflected in them appearing at different regions in the NMR spectrum. Thus, for the NMR active Tc-99 nucleus, the odd oxidation states of +1, +3, +5, and +7 are particularly suitable for NMR spectroscopy. More importantly, the most abundant oxidation state of +7 of low spin Tc-99 nucleus, which is common in environmental samples under oxic environments, has a distinct Tc-99-NMR chemical shift at 0 ppm, with a small line width (~25 Hz) (Levitskaia et al. 2014). Tc-99 in the +7 oxidation state is expected to be the dominant form found in the resin samples.

For the NMR experiment, 3 mL of the liquid supernatant in contact with the resins were aliquoted, and their Tc-99 NMR spectra were collected. Both the solutions show a single resonance at 0 ppm, corresponding to the presence of a single Tc-99 environment assigned to TcO_4^- . The NMR intensity per scan of the supernatant in contact with the heat-treated resin was observed to be 200% that of the supernatant in contact with the untreated resin, as shown in Figure 5. This suggests the presumable greater loss of Tc in the form of TcO_4^- from the resin under heat treatment.

The Tc-99 NMR spectrum of the rinsed B37FR2 resin (Figure 5B, black trace) shows a broad resonance at 10 ppm attributed to the TcO_4^- bound to the hydrophobic trihexylammonium exchange sites on the resin. This resonance overlays with the broad TcO_4^- resonance observed for the pristine Purolite A530E resin loaded with 0.02 M TcO_4^- from DIW, confirming the presence of the Tc in +7 oxidation state present on the resin. A weak broad resonance at about -18 ppm suggests presence of Tc(VII) in the different chemical environment on the resin, possibly TcO_4^- bound to the triethylammonium exchange sites. The exact determination is difficult due to the poorly defined spectral profile of this resonance.

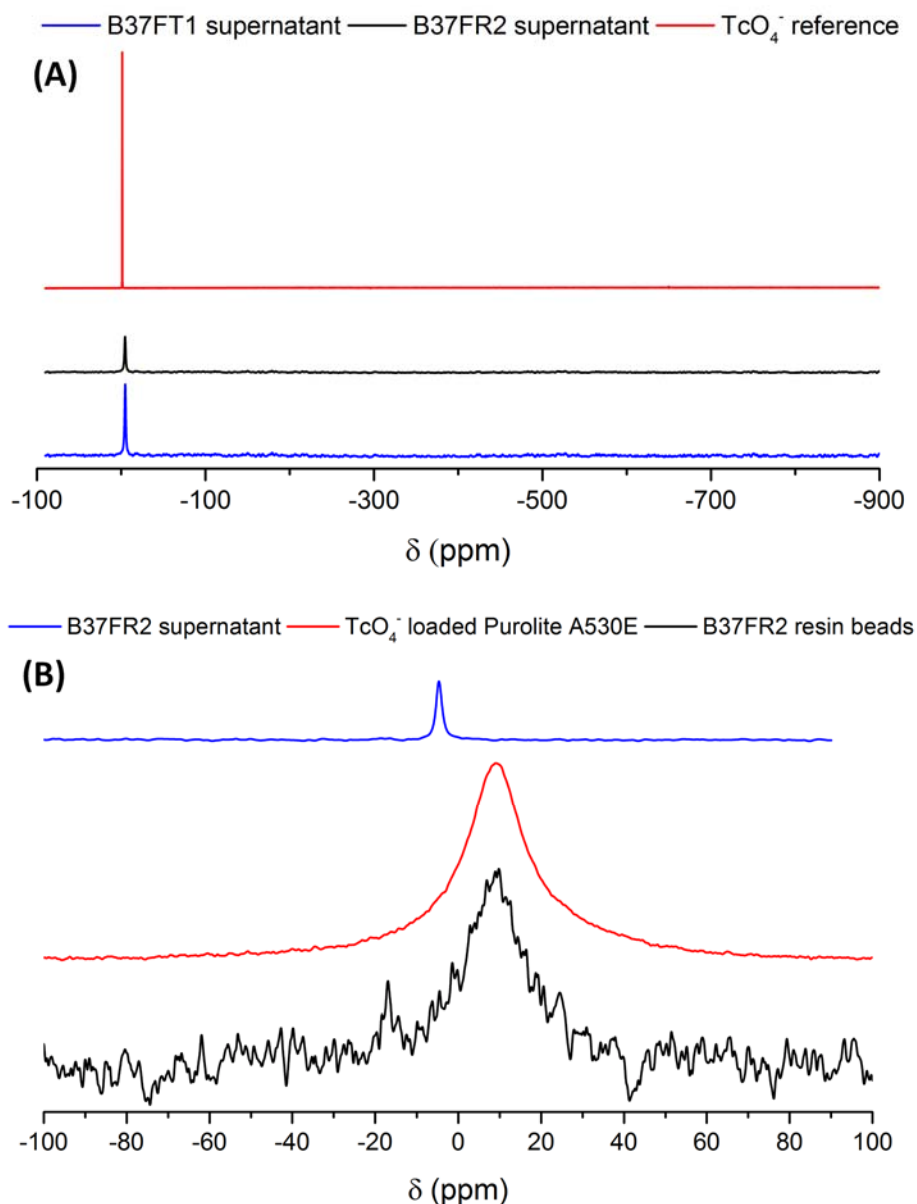


Figure 5. (A) Solution state Tc-99 NMR spectra per scan of the supernatants in contact with B37FT1 (blue trace) heat-treated resin and B37FR2 (black trace) untreated resin. (B) Tc-99 NMR spectra per scan of B37FR2 resin beads thoroughly rinsed with deionized water to remove any interstitial liquid compared to B37FR2 supernatant.

The Tc-99 NMR experiment on the hydrated B37FR2 resin (~3 mL) is shown in Figure 2 with spectra plotted as intensity per scan. These beads were removed from the supernatant and washed thoroughly with DIW to remove any interstitial liquid and loaded into a capped PTFE/FEP copolymer sleeves, which were then inserted into 5- or 10-mm glass NMR tubes. There appear to be two different TcO_4^- environments in the resin. One resonance appears at -0.5 ppm with a relatively sharp profile and the other displays a broad profile centered about 10 ppm. The overlaid spectrum from B37FR2 supernatant can be used to assign the -0.5 ppm resonance to the hydrated TcO_4^- , similar to the TcO_4^- in solution and likely to be associated with the hydrophilic triethylammonium IX site, whereas the resonance at 10 ppm is likely

non-hydrated TcO_4^- tightly bound to the hydrophobic trihexylammonium, resulting in the broadened signal.

4.1.3 EPR Spectroscopy

The EPR spectrum of the B37FR2 resin sample collected at 125 K shows a broad unresolved signal, which maintains its general profile albeit at reduced intensity at lower temperatures (Figure 6A). Similar spectral profile was observed for the B37FT2 resin (Figure 6B). The obtained spectra at 7-125 K lack fine structure and are not resolved into 10-line multiple characteristic for Tc(II, VI) species; reference spectrum of Tc(VI) is shown in Figure 6C for comparison. Further, reducing temperature to 2-4 K did not lead to the appearance of new spectral feature, indicating the absence of the Tc(IV) species retained by the resin; the reference Tc(IV) spectrum is shown in Figure 6D. The observed EPR signal generated by the resin samples was attributed to the overlapping spectra generated by the paramagnetic Fe, Cr, Co, and other transition metals retained by the resin, as is evident from the direct analysis of the resin beads by EDX (see Section 4.1.5) and the results of the elemental analysis using digested resin samples (see Section 4.1.7).

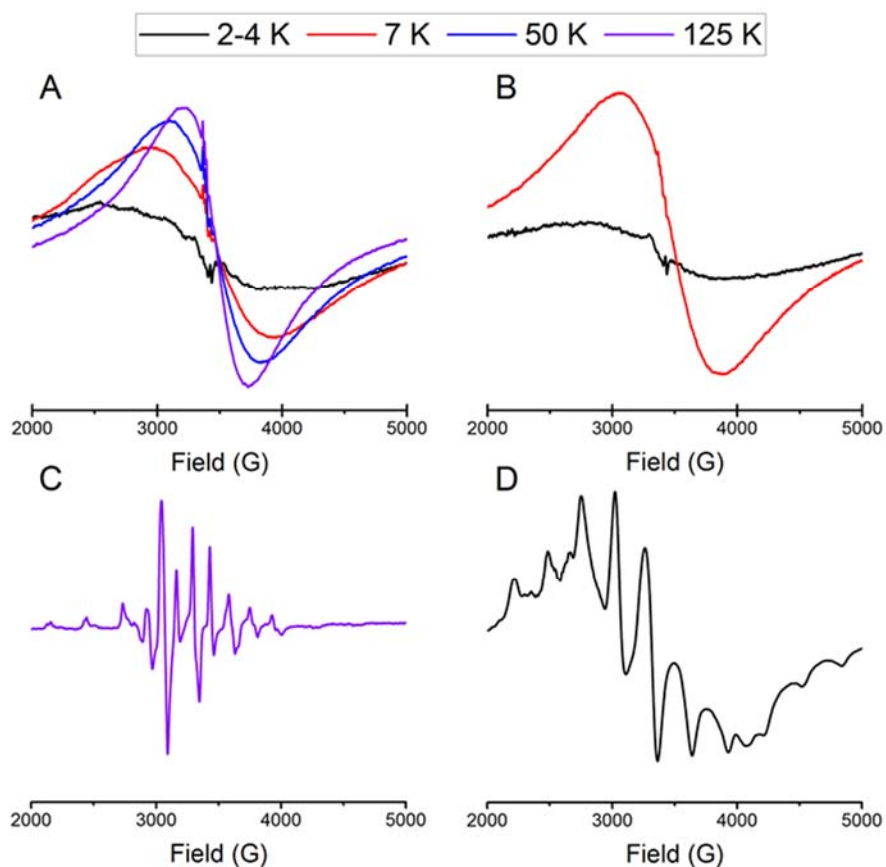


Figure 6. EPR spectra acquired at variable temperatures for (A) B37FR2 resin; (B) B37FT1 resin; (C) Tc(VI) reference (TcO_4^{2-}); and (D) Tc(IV) reference ($\text{TcO}_2 \cdot x\text{H}_2\text{O}$) obtained by electrochemical reduction of 10 mM TcO_4^- in 5.0 M NaNO_3 , 2 M NaOH solution. Reference spectra are taken from Chatterjee et al. 2017.

4.1.4 Scanning Electron Microscopy

SEM is useful for gaining information about a sample's surface topography and composition. A whole resin bead was observed under the microscope and the resulting image is shown in Figure 7A. The resin bead appears as a smooth, uniform sphere with a diameter of approximately 600 μm . Figure 7B represents a cross section of a resin bead cut using a razor blade. It is apparent that the razor blade did not produce a clean cut, as there are indentations and imperfections on the face of the cross-sectioned bead.

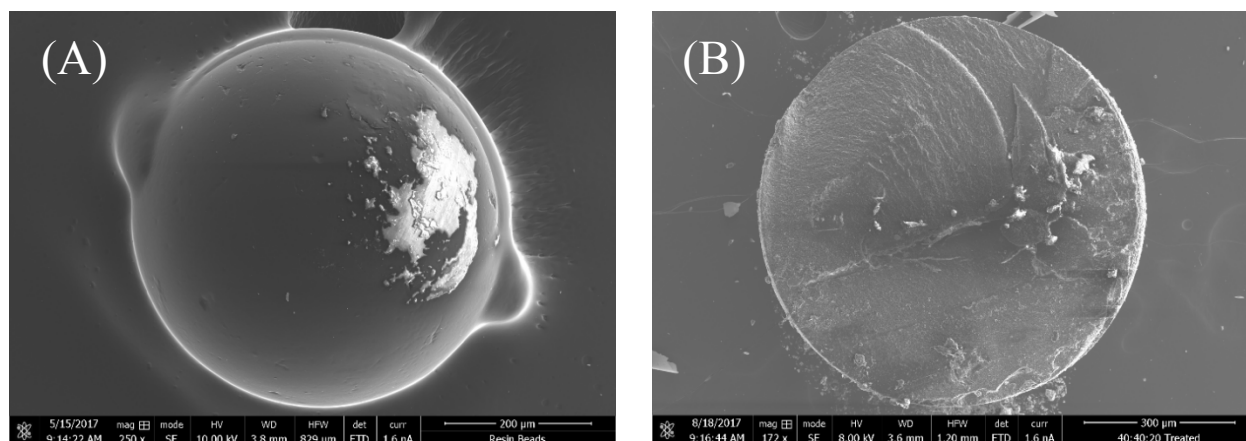


Figure 7. SEM images of (A) B37FR2 resin bead and (B) cross section of B37FR2 resin bead cut using a razor blade.

4.1.5 Energy-Dispersive X-ray Spectroscopy

EDX was used in combination with SEM to determine elemental composition on the surface of three different-colored resin beads from the untreated B37FR2 resin sample. A minimum of five spectra were collected on the surface of each resin bead, and the average mass percent of each element is listed in Table 1 with corresponding relative standard deviations (%RSD).

Table 1. Average mass percent of elements present on the surface of an orange, tan, and off-white resin bead collected from untreated B37FR2 determined by energy dispersive X-ray spectroscopy.

Average atomic percent of elements and relative standard deviation (%RSD) for the whole B37FR2 beads											
	Element	C	O	Al	Si	P	S	Cl	Ca	Cr	Fe
Orange bead	Average mass %	67	28	-	1.0	0.2	0.1	0.2	0.1	0.4	3.4
	% RSD	11%	23%	-	49%	26%	13%	18%	21%	7%	12%
Tan bead	Average mass %	75.5	20	0.19	1.5	-	0.93	0.15	0.09	1.2	0.39
	% RSD	3%	19%	29%	34%	-	41%	52%	45%	57%	43%
Off-white bead	Average mass %	82.3	16.9	-	-	-	0.22	0.13	-	0.25	-
	% RSD	1%	5%	-	-	-	6%	9%	-	6%	-

The resin beads are manufactured using a polystyrene base, which is responsible for carbon being present as the largest constituent by mass. Similarly, most of the oxygen present is likely due to residual water. Chromium, which is one of the contaminants of concern for groundwater at the Hanford Site, is present on the surface of all resin beads analyzed. This confirms that chromium is retained by the Puralite A530E resin as Cr(VI) in the form of chromate or dichromate anion. The chromium mass percent of the cross-sectioned bead also aligns well with the surface characterization of the resin beads, where the tan-colored bead had the highest chromium content at 1.2% and 1.3% for surface and cross section analysis, respectively.

An increasing amount of iron is present on the surface of the resin bead as the color darkens from off-white to orange. There is no detectable iron in the off-white bead, but nearly 3.5% of the total elemental composition is attributed to iron for the orange bead, likely the largest contributor to the difference in colors. One bead of each color (off-white, tan, and orange) was cross-sectioned and analyzed by EDX to map elemental composition adsorbed into the beads. The EDX intensity of each element as a function of the surface position on the resin bead can be seen in Figure 8. The horizontal green line across the bead surface represents the scan path and the corresponding intensities of elements observed at each position are highlighted by the colored lines. The most notable observation is the spikes in iron intensity as the bead is scanned. It is unclear if the spikes are inherent to the bead or are a result of contamination from the razor blade used to cross-section the beads. Regardless, the cumulative results across all regions of the cross-sectioned beads shown in Table 2 indicate that the iron content is highest for the cross-sectioned orange bead, consistent with the EDX measurements performed on the surface of the beads.

Among non-metal elements, sulfur and chlorine were found on the resin, most likely retained as sulfate and chloride anions.

No technetium was observed by EDX in any of the beads analyzed. Tc-99 has an emission X-ray at 18.37 keV, which was within the energy range scanned for EDX (Bearden 1967). This leads to the conclusion that the Tc-99 concentration is too low for detection by EDX.

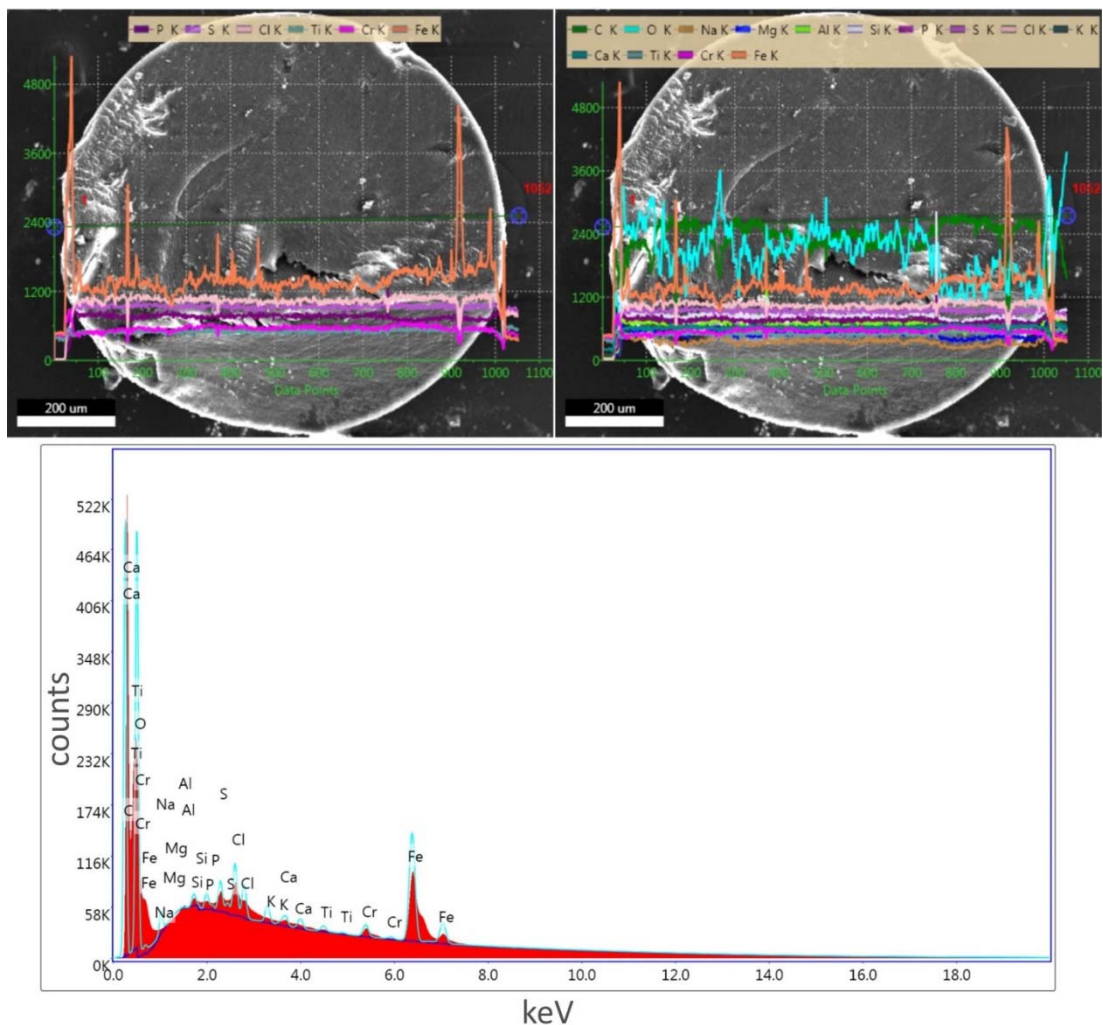


Figure 8. Straight line EDX along the cross-sectioned surface of an orange resin bead. The top left displays the frequency of select elements as the scan progresses across the bead. The top right displays the same information for all elements observed. The graph on the bottom shows the cumulative EDX spectrum across all regions of the cross-sectioned bead.

Table 2. Average mass percent of elements observed by EDX while scanning across the surface of cross-sectioned resin beads of varying color for untreated B37FR2 resin.

Average atomic percent of elements for the sectioned B37FR2 beads													
Element	C	O	Na	Mg	Si	P	S	Cl	K	Ca	Ti	Cr	Fe
Orange Bead	46.2	47.2	0.5	0.0	0.1	0.2	0.4	0.7	0.2	0.2	0.1	0.3	4.0
Tan Bead	45.3	48.7	0.6	0.0	0.2	0.2	0.8	0.9	0.2	0.3	0.1	1.3	1.5
Off-white bead	47.0	45.1	3.0	0.2	0.3	0.1	0.5	1.2	0.2	0.4	0.1	0.4	1.6

4.1.6 GEA Results

One non-destructive assay technique to quantify radionuclides in a sample is through a combination of GEA using an HPGe detector and LEPS. HPGe detectors are useful for analyzing gamma energies greater than 46 keV, but cannot quantify gamma and X-rays below 40 keV, which is done by LEPS.

Results from GEA indicate Co-60 and Tc-99 are present in both the temperature-treated and untreated resin samples from the 200 West P&T facility. The activities of these radionuclides and their associated concentrations are given in Table 3. This is in agreement with a previous report where the Co-60 concentration on the resin was at 475 pCi/g (Valenta et al. 2010).

Table 3. Activities and associated concentrations of radionuclides retained by temperature-treated and untreated Purolite A530E resin quantified by GEA. The results are expressed in Bq or μg nuclide per gram of hydrated resin.

Sample	Co-60			Tc-99		
	Bq/g	% RSD	$\mu\text{g/g}$	Bq/g	% RSD	$\mu\text{g/g}$
B37FR2	1.35	2%	3.2E-08	1.32E+04	10%	18.9
B37FT1	1.58	1%	3.8E-08	1.20E+04	5%	20.8

A low energy X-ray peak was observed at 39.6 keV in the HPGe spectrum, which led to inquisition of I-129 present in the sample. In order to measure I-129 quantitatively with confidence, it was necessary to use LEPS to analyze the low-energy X-rays. The LEPS spectrum for resin B37FR2 along with corresponding X-ray energies is shown in Figure 9. The relatively higher energy 89.5 keV gamma from Tc-99 is plainly evident along with X-rays at 19.2 and 21.6 keV, which are a combination of Tc-99 emissions. Also present in the spectrum are lines attributable to I-129 with the most prominent peak at 29.7 keV with a roughly 55% total yield. This line, in combination with the X-ray peak at 33.61 keV, was used to quantify the concentration of I-129 sorbed to the resin. The X-ray at 39.58 keV was excluded from analysis due to the high experimental uncertainty in the integration.

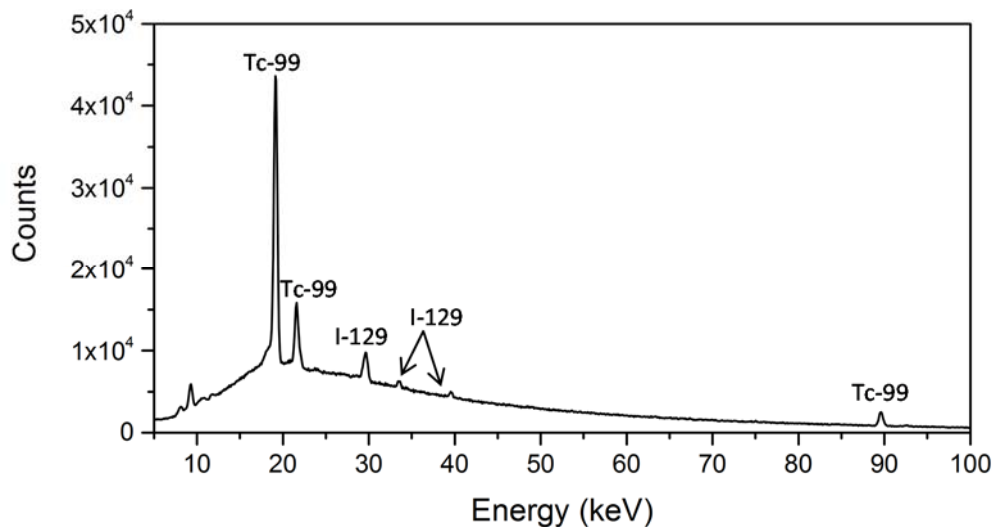


Figure 9. LEPS spectrum of B37FR2 untreated resin with corresponding X-ray energies from Tc-99 and I-129 present within the sample.

There is very good agreement between the Tc-99 results from the LEPS and GEA counts using the 89.5 keV gamma, with slightly better relative uncertainty for the activity measured by the LEPS detector as shown in Table 4. The lower energy Tc-99 X-ray peaks report higher intensities in both samples than the 89.5 keV gamma ray peak. Upon examination of Figure 9, it is obvious that the X-rays at both 19.2 and 21.6 keV have contributions from interfering X-ray emissions that result in artificially inflated Tc-99 activities. Nonetheless, the agreement between the GEA and LEPS activities for Tc-99 at 89.5 keV instills confidence in the I-129 activity measured from the 29.7 keV X-ray.

Table 4. LEPS spectrum analysis for I-129 and Tc-99 for temperature-treated (B37FT1) and untreated (B37FR2) resin samples in a 10-mL count geometry. The results are expressed in Bq or μg nuclide per gram of hydrated resin.

Sample	I-129				Tc-99			
	Line (keV)	Bq/g	% RSD	$\mu\text{g/g}$	Line(keV)	Bq/g	% RSD	$\mu\text{g/g}$
B37FR2	29.7	3.83E-01	4.2%		19.15 ^(b)	7.33E+05	0.6%	
	33.61	4.12E-01	13.6%	0.061	21.63 ^(b)	8.54E+05	1.6%	20.5
	39.58 ^(a)	2.63E-01	18.7%		89.5	1.30E+04	4.7%	
B37FT1	29.7	4.21E-01	4.1%	0.063	19.15 ^(b)	7.90E+05	0.5%	
	33.61	4.05E-01	5.9%		21.63 ^(b)	8.98E+05	1.8%	21.9
	39.58 ^(a)	2.44E-01	18.4%		89.5	1.39E+04	3.5%	

(a) X-ray line excluded from quantification of I-129 due to high experimental uncertainty.

(b) The higher activity calculated from the low-energy Tc-99 X-rays can be attributed to overlap of those lines with an interfering X-ray, which leads to artificially high activities. The line at 89.5 keV agrees well with the Tc-99 activity calculated using GEA.

The concentration of Tc-99 is orders of magnitude greater than either Co-60 or I-129 sorbed onto the IX resin; however, both Co-60 and I-129 are quantifiable by non-destructive radiometric counting. The I-129 concentration is about 350 times less than that of the Tc-99 concentration loaded onto the Purolite A530E resin. Also, there is no statistical difference between the concentration of Tc-99 retained by the resin after temperature treatment and that of the untreated resin sample as analyzed by GEA and LEPS.

4.1.7 Destructive Analysis of Resin Samples

A destructive wet oxidation method was employed to strip metals and specific radionuclides of interest, Tc-99 and U-238, from resin samples for analysis by ICP-OES and ICP-MS. The two resin samples underwent the same wet oxidative treatment in duplicate, along with commercially available Purolite A530E resin as a control, and the average concentrations and relative standard deviations are shown in Table 5.

The results indicate that several metals sorb to the resin along with technetium, most notably, chromium, cobalt, and iron. Chromium is one of the contaminants of concern for Hanford groundwater plumes, and it appears to be present in approximately 50-fold excess of Tc-99 concentration on both the temperature-treated resin and untreated resin, with slightly higher concentrations observed for the temperature-treated resin. This is in excellent agreement with the EDX results for Cr found between 0.3 and 1.3 mass percent based on the resin bead selected.

Table 5. ICP-OES results for the pristine Purolite A530E in comparison to the temperature-treated B37FT1 resin and the untreated B37FR2 resin as received from the 200 West P&T facility post wet-oxidation treatment.

	Elemental composition reported as $\mu\text{g/g}$ of resin					
	Purolite A530E	% RSD	B37FR2	%RSD	B37FT1	%RSD
Aluminum	120	11%	45	4%	142	8%
Barium	107	28%	103	3%	248	5%
Boron	458	27%	230	4%	441	12%
Calcium	18,054	0%	12847	41%	21438	1%
Chromium	ND	-	719	0%	1000	3%
Cobalt	ND	-	4.8	2%	5	8%
Iron	34	20%	1146	8%	1386	3%
Magnesium	94	7%	71	32%	119	1%
Manganese	1	14%	ND	-	1	13%
Phosphorus	44	14%	66	22%	106	2%
Potassium	124	21%	25	141%	96	16%
Silicon	947	117%	1128	36%	3866	5%
Sodium	1250	49%	469	8%	1045	20%
Strontium	19	12%	15	31%	23.6	4%
Sulfur	2082	7%	1619	13%	2976	6%
Titanium	3	71%	174	140%	180	127%
Zinc	1927	8%	1361	38%	2280	3%
Zirconium	ND	-	0.3	141%	0.8	11%
Tc-99 ^(a)	ND	-	16.7	7%	22.0	5%
U-238 ^(a)	0.06	2%	7.6	2%	11	9%
I-127 ^(a)	0.4	44%	44	9%	58	10%

(a) Analyzed by ICP-MS

The concentration of iron retained by the Purolite A530E resin was significant. The B37FT1 sample contained slightly more iron than B37FR2, but both samples had concentrations upward of 1 mg Fe/gram of resin. This is more than 5 times the concentration of Tc-99 sorbed onto the Purolite resin. The presence of iron is likely the largest contributor to the change in the color of the beads, as suggested in EDX.

The high concentration of zinc, sulfur, sodium, calcium, and boron in the control Purolite A530E sample likely originates from preparation and processing of the resin framework. ICP-OES results of these elements show concentrations in the spent B37FR2 and B37FT1 samples at or below the concentration of these elements in the pristine Purolite A530E resin that served as a control.

Based on the ICP-MS results, Tc-99 concentration on the B37FT1 resin of 16.7 $\mu\text{g/g}$ was slightly higher than that in the B37FR2 resin at 22.0 $\mu\text{g/g}$. The latter value is in excellent agreement with both GEA and LEPS results; converting the radioactivity of Tc-99 determined using these techniques, the total concentration of Tc-99 on the temperature-treated resin was found to be 21.9 $\mu\text{g/g}$ of resin. The concentration of Tc-99 in the untreated resin by GEA and LEPS was calculated to be 20.5 $\mu\text{g/g}$ and is in

satisfactory agreement with the ICP-MS result of 16.7 $\mu\text{g/g}$. The uniformity of the resin is likely presenting some challenges in analytical quantification of metals by the destructive technique where the sample size is so much smaller (250 mg) compared to the nominal 10 g of sample analyzed by GEA and LEPS. This is likely contributing to some discrepancy between the Tc-99 concentrations determined for the untreated resin from the two different techniques, although the sample is said to be homogenous.

Uranium-238 was also quantified by ICP-MS and concentrations of uranium were approximately half the concentration of Tc-99 at 11 and 7.6 $\mu\text{g/g}$ of resin for the B37FT1 and B37FR2 samples, respectively.

Results of ICP-MS for non-radioactive I-127 indicate that a significant amount of iodine is retained by the resin. The concentration of iodine was found to be 3 times that of the technetium concentration on the resin at 58 and 48 $\mu\text{g/g}$ of resin for B37FT1 and B37FR2, respectively. There were detectable concentrations of iodine in the bubbler solutions during the dissolution process, as shown in Table 6, whereas the Tc-99 concentration was non-detectable. Iodine species are volatile, especially in acidic solutions; thus the concentration in the bubbler solutions is non-negligible as observed by ICP-OES. It is also important to note that substantial concentrations of both iodine and technetium are detected in the second dissolution step. Comparing the concentration of I-129 determined by LEPS with the I-127 concentration from ICP-MS indicates that the amount of I-127 on the spent resin is approximately 1000 times greater than that of I-129.

Table 6. ICP-MS results for sequential dissolution of B37FR2 and B37FT1 resin for Tc-99 and I-129.

		Concentration of Tc-99 and I-127 reported as $\mu\text{g/g}$ of resin							
		First Dissolution				Second Dissolution			
		B37FR2		B37FT1		B37FR2		B37FT1	
		Resin	Bubbler	Resin	Bubbler	Resin	Bubbler	Resin	Bubbler
Tc-99	Average	12.6	0.05	16	ND	4	0.01	5.7	ND
	%RSD	1%	71%	7%	-	33%	71%	0%	-
I-127	Average	32	3	44	0.5	8	0.8	13	0.4
	%RSD	21%	62%	7%	55%	10%	1%	14%	79%

4.1.8 IO_3^- and IO_4^- uptake by Purolite A530E

To evaluate iodine retention on the resin, Raman spectroscopy was utilized to monitor the concentration of IO_3^- and IO_4^- in the solutions contacted with the pristine Purolite A530E resin to investigate sorption behavior of iodate and periodate. The percent uptake for each analyte can be calculated by measuring the inverse ratio of intensities of the initial solution and the resulting intensity of the Raman stretch after contact with Purolite A530E, as shown in Eq. (1).

$$\% \text{ uptake} = \frac{(\text{Intensity of Raman band in solution after contact})}{(\text{Intensity of Raman band in initial solution})} \times 100 \quad (1)$$

The Raman spectra of 0.02 M KIO_3 and 0.02 M KIO_4 before and after contact with Purolite A530E resin is shown in Figure 10. Iodate uptake was calculated using the peak at 800.44 cm^{-1} as shown in Figure 10A. This resulted in iodate uptake of 26% after 10 minutes of contact with the pristine Purolite resin. Periodate, which exhibits tetrahedral geometry and is chemically similar to both TcO_4^- and ClO_4^- , for which Purolite A530E is selective, exhibited highly efficient uptake of 91% as determined by using vibration band at 792.43 cm^{-1} . It should be noted that in this experiment, the total amount of IO_3^- or IO_4^- in the system was 0.02 meq while the amount of resin used in each experiment (50 mg) contained 0.03 meq of the theoretical active sites, resulting in only marginal excess. This suggests that under the column conditions where the resin active sites are present in the large excess relative to the analyte, much more efficient uptake of iodate is expected. This is significant finding since iodate dominates speciation of iodine in the Hanford groundwater (Zhang and Hou 2013).

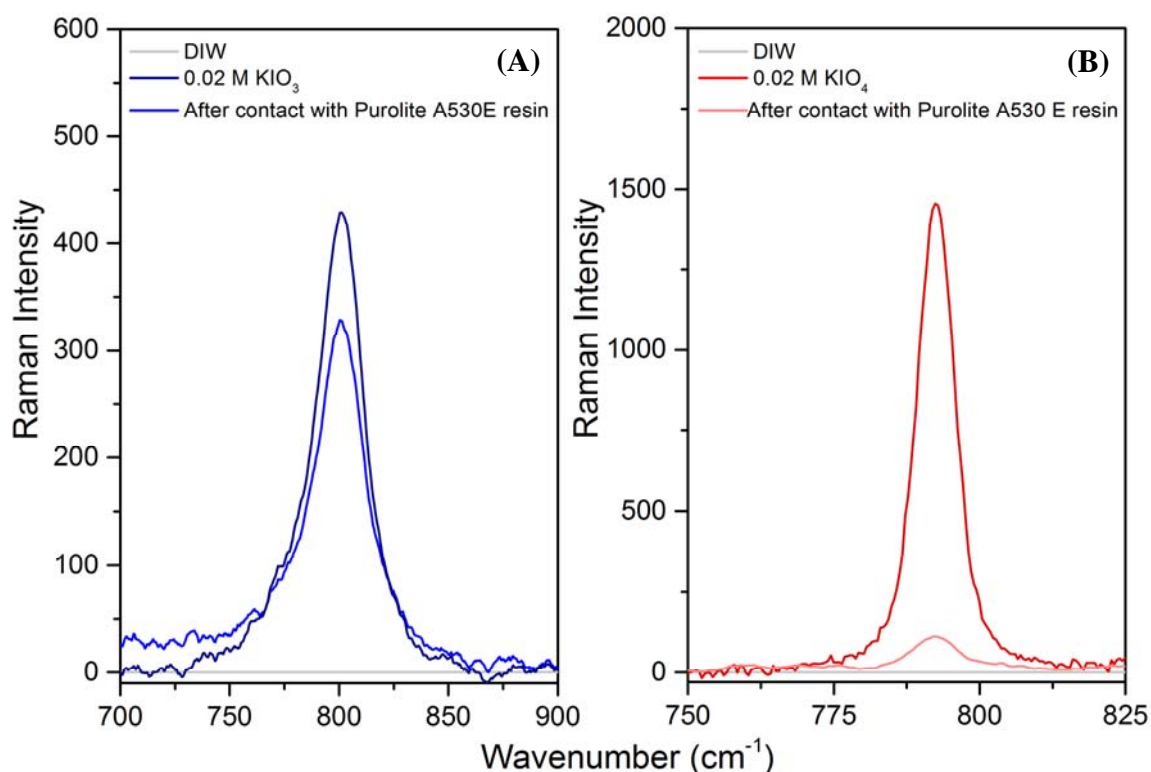


Figure 10. Raman spectroscopy of (A) 0.02 M KIO_3 and (B) 0.02 M KIO_4 in contact with 50 mg of Purolite A530E resin.

5.0 Quality Assurance

The PNNL Quality Assurance (QA) Program is based upon the requirements as defined in the DOE Order 414.1D, *Quality Assurance*, and 10 CFR 830, *Energy/Nuclear Safety Management*, Subpart A – Quality Assurance Requirements. PNNL has chosen to implement the following consensus standards in a graded approach:

- ASME NQA-1-2000, *Quality Assurance Requirements for Nuclear Facility Applications*, Part 1, Requirements for Quality Assurance Programs for Nuclear Facilities.
- ASME NQA-1-2000, Part II, Subpart 2.7, Quality Assurance Requirements for Computer Software for Nuclear Facility Applications, including problem reporting and corrective action.
- ASME NQA-1-2000, Part IV, Subpart 4.2, Guidance on Graded Application of Quality Assurance (QA) for Nuclear-Related Research and Development.

The procedures necessary to implement the requirements are documented through PNNL's “How Do I...? (HDI), a system for managing the delivery of laboratory-level policies, requirements and procedures.

The *DVZ-AFRI Quality Assurance Plan* (QA-DVZ-AFRI-001) is the minimum applicable QA document for Deep Vadose Zone – Applied Field Research Initiative (DVZ-AFRI) projects under the NQA-1 QA program. This QA Plan also conforms to the QA requirements of DOE Order 414.1D and 10 CFR 830, Subpart A. The DVZ-AFRI is subject to the *Price Anderson Amendments Act*.

The implementation of the DVZ-AFRI quality assurance program is graded in accordance with NQA-1-2000, Part IV, Subpart 4.2, Guidance on Graded Application of Quality Assurance (QA) for Nuclear-Related Research and Development.

Three technology levels are defined for this DVZ-AFRI QA Program:

- **Basic Research** consists of research tasks that are conducted to acquire and disseminate new scientific knowledge. During basic research, maximum flexibility is desired in order to allow the researcher the necessary latitude to conduct the research.
- **Applied Research** consists of research tasks that acquire data and documentation necessary to assure satisfactory reproducibility of results. The emphasis during this stage of a research task is on achieving adequate documentation and controls necessary to be able to reproduce results.
- **Development Work** consists of research tasks moving toward technology commercialization. These tasks still require a degree of flexibility and there is still a degree of uncertainty that exists in many cases. The role of quality on development work is to make sure that adequate controls to support movement into commercialization exist.

Research and Development Support Activities are those that are conventional and secondary in nature to the advancement of knowledge or development of technology, but allow the primary purpose of the work to be accomplished in a credible manner. An example of a support activity is controlling and maintaining documents and records. The level of quality for these activities is the same as for Developmental Work.

Within each technology level, the application process for QA controls is graded such that the level of analysis, extent of documentation, and degree of rigor of process control are applied commensurate with their significance, importance to safety, life cycle state of a facility or work, or programmatic mission. The work for this report was performed under the technology level of Basic Research.

The project used PNNL's Environmental Sciences Laboratory (ESL) for chemical analyses required as part of laboratory and field experiments and testing. The ESL operates under a dedicated quality assurance plan that complies with the *Hanford Analytical Services Quality Requirements Document* (HASQARD), DOE/RL-96-68, Rev. 3 (DOE-RL 2007b). ESL implements HASQARD through *Conducting Analytical Work in Support of Regulatory Programs* (CAWSRP). Data Quality Objectives established in CAWSRP were generated in accordance with HASQARD requirements. Chemical analyses of testing samples and materials were conducted under the ESL QA Plan.

6.0 Conclusions

Overall, while nearly 6 Ci of Tc-99 has been removed from groundwater over three years of operation, analysis of the spent P&T Purolite A530E resin shows that Tc-99 loading is small and constitutes only about 0.034% of the theoretical capacity of the resin. However, an appreciable quantity of iodine is retained on the resin, as is evident from both I-127 ICP-MS and I-129 LEPS measurements. The concentrations of I-127 and I-129 on the resin were found to be about 2.5 times greater and 350 times smaller than that of Tc-99, respectively. This means that a significant amount of non-radioactive iodine is being retained on the resin, and radioactive iodine to a much lesser extent. The concentration ratio of I-127 to I-129 on the resin is about 1000 and is consistent between B37FR2 and B37FT1. This may be representative of the low concentration of radioactive I-129 in the groundwater relative to the total iodine in groundwater. A preliminary control experiment confirmed retention of iodate by the Purolite A530E resin by Raman spectroscopy. Further testing is warranted to investigate efficiency and selectivity of iodate retention.

Small quantities of Co-60 and U-238 were also found on the resin. Other contaminants retained on the resin in significant quantities included chromium and iron. Resin beads were found to be inhomogeneous by EDX, with a significant concentration of iron present in some fraction of the resin beads. Iron-loaded resin beads could be easily identified by their distinct orange color, which was most likely due to the Fe(III) hydroxide. Additional studies are warranted to examine whether sorbed iron interferes with TcO_4^- retention by the Purolite A530E resin.

Analytical ICP-MS results for Tc-99 obtained using resin wet oxidation method are in excellent agreement with non-destructive radiometric counting techniques. Average Tc-99 concentrations in the resin samples calculated using results of these three techniques are 19 ± 2 and 21.6 ± 0.7 for B37FR1 and B37FT1, respectively. These values are the same within observed experimental error and indicate that the thermal treatment of the resin performed to remove halogenated organics from the loaded resin does not result in the leaching of Tc-99 from the resin.

7.0 References

- 10 CFR 830, *Energy/Nuclear Safety Management*. Code of Federal Regulations, as amended.
- ASME NQA-1-2000, *Quality Assurance Requirements for Nuclear Facility Applications*. American Society of Mechanical Engineers, New York, NY.
- Bearden JA. 1967. "X-Ray Wavelengths." *Rev. Mod. Phys.* 39(1):78–124.
- Bonnesen PV, GM Brown, SD Alexandratos, LB Bavoux, DJ Presley, V Patel, R Ober, and BA Moyer. 2000. "Development of Bifunctional Anion-Exchange Resins with Improved Selectivity and Sorptive Kinetics for Per technetate: Batch-Equilibrium Experiments." *Environ. Sci. Technol.* 34(17):3761–3766.
- Breedlove WM, J Morse, A Tortoso, K Martins, M Byrnes, and S Simmons. 2011. "Groundwater Pump and Treat Remediation System Overview, Hanford 200-West Area – 11508." 2011 Waste Management Symposia, February 27–March 3, 2011, Phoenix, AZ.
- Chatterjee S, A Andersen, Y Du, MH Engelhard, GB Hall, TG Levitskaia, WW Lukens, V Shutthanandan, ED Walter, and NM Washton. 2017. *Characterization of Non-Per technetate Species Relevant to the Hanford Tank Waste*. PNNL-26265; EMSP-RPT-035, Pacific Northwest National Laboratory, Richland, WA.
- Cho H, WA De Jong, BK McNamara, BM Rapko, and IE Burgeson. 2004. "Temperature and Isotope Substitution Effects on the Structure and NMR Properties of the Per technetate Ion in Water." *J. Am. Chem. Soc.* 126(37):11583–11588.
- DOE-RL. 2007a. *Treatability Test Plan for Using Purolite Resin to Remove Technetium-99 from 200-ZP-1 Groundwater*. DOE/RL-2006-64, Rev. 0, U.S. Department of Energy, Richland Operations Office, Richland, WA.
- DOE-RL. 2007b. *Hanford Analytical Services Quality Requirements Document*. DOE/RL-96-68, Rev. 3, U.S. Department of Energy, Richland Operations Office, Richland, WA.
- DOE Order 414.1D, *Quality Assurance*. U.S. Department of Energy, Washington, D.C.
- Dorr KA, JR Freedman-Pollard, and MJ Ostrom. 2013. *Lessons Learned from the 200 West Pump and Treatment Facility Construction Project at the US DOE Hanford Site - A Leadership for Energy and Environmental Design (LEED) Gold-Certified Facility*. CHPRC-01924-FP, Rev. 1, CH2M Hill Plateau Remediation Company, Richland, WA.
- EPA. 2007a. *Inductively Coupled Plasma-Atomic Emission Spectrometry*. EPA SW-846 Test Method 6010C, Rev. 3, U.S. Environmental Protection Agency, Washington, D.C.
- EPA. 2007b. *Inductively Coupled Plasma-Mass Spectrometry*. EPA SW-846 Test Method 6020A, Rev. 1, U.S. Environmental Protection Agency, Washington, D.C.

- Franklin KJ, C JL Lock, BG Sayer, and GJ Schrobilgen. 1982. "Chemical Applications of Technetium-99 NMR Spectroscopy: Preparation of Novel technetium(VII) Species and Their Characterization by Multinuclear NMR Spectroscopy." *J. Am. Chem. Soc.* 104(20):5303–5306.
- Gu B, GM Brown, and CC Chiang. 2007. "Treatment of Perchlorate-Contaminated Groundwater Using Highly Selective, Regenerate Ion-Exchange Technologies." *Environ. Sci. Technol.* 41(17):6277–6282.
- Gu B, YK Ku, and GM Brown. 2005. "Sorption and Desorption of Perchlorate and U(VI) by Strong-Base Anion-Exchange Resins." *Environ. Sci. Technol.* 39(3):901–907.
- Lee, H, B Lee, M. Carlson, J. Geiger, D Saunders, K Bral, E Cordova, M Niebauer, B Christiansen. 2017. Characterization and Well Remediation Strategies for Improved Long-term Pump and Treat System Injection Well Performance. Paper 17272. Waste Management 2017 Symposium Proceedings. Phoenix, AZ. March 2017.
- Levitskaia TG, A Andersen, SD Chatterjee, HM Cho, JM Peterson, BM Rapko, ED Walter, and NM Washton. 2014. *Speciation and Oxidative Stability of Alkaline Soluble, Non-Perchnetate Technetium*. PNNL-23654; EMSP-RPT-024, Rev. 0, Pacific Northwest National Laboratory, Richland, WA.
- Lukens WW, JJ Bucher, NM Edelstein, and DK Shuh. 2002. "Products of Perchnetate Radiolysis in Highly Alkaline Solution: Structure of $TcO_2 \cdot xH_2O$." *Environ. Sci. Technol.* 36(5):1124–1129.
- Odom B, D Hanneke, B D'Urso, and G Gabrielse. 2006. "New Measurement of the Electron Magnetic Moment Using a One-Electron Quantum Cyclotron." *Phys. Rev. Lett.* 97(3):030801–030801.
- PNNL. 2016a. *Inductively Coupled Plasma-Optical Emission Spectrometry (ICP-OES) Analysis*. Technical Procedure PNNL-ESL-ICP-OES, Rev. 4, Pacific Northwest National Laboratory, Richland WA.
- PNNL. 2016b. *Inductively Coupled Plasma Mass Spectrometry (ICP-MS) Analysis*. Technical Procedure PNNL-ESL-ICPMS, Rev. 4, Pacific Northwest National Laboratory, Richland WA.
- Rehr JJ, RC Albers, and SI Zabinsky. 1992. "High-Order Multiple-Scattering Calculations of X-Ray-Absorption Fine Structure." *Phys. Rev. Lett.* 69(23):3397–3400.
- Stoll S and A Schweiger. 2006. "EasySpin, a comprehensive software package for spectral simulation and analysis in EPR." *J. Magn. Reson.* 178(1):42–55.
- Valenta MM, KE Parker, and EM Pierce. 2010. *Tc-99 Ion Exchange Resin Testing*. PNNL-19681, Pacific Northwest National Laboratory, Richland, WA.
- Zhang LY and XL Hou. 2013. "Speciation Analysis of I-129 and its Applications in Environmental Research." *Radiochim Acta* 101:525-540.

Distribution

**No. of
Copies**

Name
Organization
Address
City, State and ZIP Code

Organization
Address
City, State and ZIP Code
Name
Name
Name
Name
Name (#)

Name
Organization
Address
City, State and ZIP Code

**No. of
Copies**

Foreign Distribution

Name
Organization
Address
Address line 2
COUNTRY

Local Distribution

Pacific Northwest National Laboratory
Name Mailstop
Name Mailstop
Name Mailstop
Name Mailstop
Name (PDF)



Pacific Northwest
NATIONAL LABORATORY

*Proudly Operated by **Battelle** Since 1965*

902 Battelle Boulevard
P.O. Box 999
Richland, WA 99352
1-888-375-PNNL (7665)

U.S. DEPARTMENT OF
ENERGY

www.pnnl.gov